

Gravitational influence of high power laser pulses

Paul Lageyre,* Emmanuel d'Humières, and Xavier Ribeyre

CEntre Laser Intenses et Applications, Univ. Bordeaux-CNRS-CEA, UMR 5107 Talence 33405, France

(Dated: June 9, 2022)

The study of gravitational wave generation in the laboratory presents an opportunity to observe and understand more easily the mechanisms at work in gravitation. The present study will focus on the gravitational deformation generated by a light pulse, as it could be generated by a current ultra-high power laser. Although of very small magnitude, the deformation thus generated has advantages over that generated by mass acceleration, and could therefore prove useful in the long-term establishment of a laboratory experiment for the generation and detection of gravitational waves.

I. INTRODUCTION

The detection of gravitational deformations limited in time is for the scientific community a chance to better understand the subtleties of the gravitational force and to confirm, or complete, its description by general relativity, theorized by Einstein between 1907 and 1915. These propagative deformations, the gravitational waves, are themselves theorized by Einstein [1].

The first gravitational waves are detected indirectly for the first time in 1974 thanks to the observations by Hulse and Taylor of a binary system of a pulsar and a neutron star, whose precession speed was affected by the radiation of a gravitational wave [2]. As for the the first direct detection, it took place at the end of 2015 [3]. It was made possible by the construction of giant interferometers such as LIGO, whose very high sensitivity has allowed the observation of changes in the length of its arms of the order of $\Delta L/L = 10^{-22}$ for frequencies on the kHz range. This new observation has rekindled the scientific community's interest in gravitational waves and what they can tell us about the physics of gravitation.

During the century that separates the prediction of gravitational waves from their observation, many methods of generating gravitational waves in the laboratory have been studied. Indeed, such a source would have the advantage of being more reproducible and adaptable to the desired observations than the observation of very intense astrophysical phenomena, even though they are more commonly observed nowadays [4]. Two approaches are favored for the generation of a large enough to be detected gravitational deformation in the laboratory. They both require powerful sources to generate a significant deformation.

The first is the explosive acceleration of a quantity of mass, which would generate a deformation of space-time through the quadrupolar acceleration of mass. This deformation can be conceived by the means of a laser striking a target ([5], [6], [7]) or in a more extreme manner by the explosion of a thermonuclear bomb [8]. The second

is the generation of a gravitational deformation by an electromagnetic wave, whose coherence is an advantage in the generation of an important deformation [9].

The observation in astrophysics of the deviation of the ray of light by Dyson and Eddington [10] constitutes one of the important tests of general relativity. This test confirms the influence the variation of the gravitational potential has on the trajectory of light in space. From the point of view of general relativity, it confirms that the deformation of space-time generated by a massive object (in this case the Sun) changes the trajectory of light which then follows the geodesic in this new space-time. From a Newtonian point of view, we can say that the Sun exerts an influence on light through the gravitational force, which implies, by reciprocity of action, that light has itself an influence on gravity. Light must therefore generate locally its own gravitational field, that is to say a deformation of space-time. The first to be interested in the gravitational deformation produced by light were Tolman, Ehrenfest and Podolsky [11] who studied the deformation generated by an infinitesimally thin ray of light on the surrounding space-time. This study of gravitational deformation by a beam of light of zero spatial extension has more recently been taken up and completed by Rätzel *et al.* [12], but the absence of a spatial extension for this beam of light prevents the complete study of gravitational deformation.

In this paper, we shall consider the generation of a gravitational deformation inside a light beam, where it should be the most important. In section 2, we will summarize linearized general relativity for small deformations of space-time, and apply it to the case of an electromagnetic wave. In section 3, we will present the analytical method used to solve this problem, and we will check the compatibility of our solution with the already known case of the Schwarzschild metric. In section 4, we will apply this calculation method to a simple model of a light pulse: the cylinder of light, of constant energy density and moving at the speed of light in vacuum c . In section 5, we will analyze the results obtained by keeping in mind the characteristics of the laser sources that could be used in a laboratory experiment. In section 6, we will summarize our results and compare them with those obtained by Ribeyre and Tikhonchuk [5], Gelfer

* paul.lageyre@u-bordeaux.fr

et al. [6] and Kadlecová *et al.* [7] in the case of a massive source. We will also mention the future developments of this paper.

II. GRAVITATIONAL DEFORMATION BY AN ELECTROMAGNETIC FIELD

We assume the existence of a plane space-time described by the Minkowsky metric $\eta_{\mu\nu} = \text{diag}(-1, 1, 1, 1)$, corresponding to the approximation of a Galilean frame of reference, where the local distance traveled on the interval ds by an object can be described as:

$$ds^2 = \eta_{\mu\nu} dx^\mu dx^\nu = -c^2 dt^2 + dx^2 + dy^2 + dz^2 \quad (1)$$

By analogy, the metric of a deformed spacetime can be written as $g_{\mu\nu}$, which can be written for a spacetime where the gravitational perturbation with respect to the planar spacetime is negligible as:

$$g_{\mu\nu} = \eta_{\mu\nu} + h_{\mu\nu} \quad (2)$$

Where $h_{\mu\nu} \ll 1$ is the perturbation in the $g_{\mu\nu}$ metric in respect to the Minkowsky metric $\eta_{\mu\nu}$.

In such a framework, Einstein's equations [14], which relate the structure of the space-time studied with the stress-energy tensor of the various elements involved, can be written as:

$$G_{\mu\nu} = \chi T_{\mu\nu} \quad (3)$$

Where $G_{\mu\nu}$ is the Einstein's tensor which describes the local space-time curvature. $T_{\mu\nu}$ is the stress-energy tensor, and $\chi = 8\pi G/c^4$ is Einstein's constant which depends on the gravitational constant G and on the speed of light in vacuum c . Applying the Lorentz gauge condition, we get:

$$\partial^\mu h_{\mu\nu} = 0 \quad (4)$$

Which gives us the linearized Einstein equations:

$$\square h_{\mu\nu} = -2\chi T_{\mu\nu} \quad (5)$$

Which are none other than d'Alembert equations, i.e. wave equations. The stress-energy tensor can be rewritten as the sum of matter's stress-energy tensor $T_{\mu\nu}^{\text{mat}}$ and electromagnetic field's stress-energy tensor $T_{\mu\nu}^{\text{em}}$.

We are interested here in the generation of a gravitational perturbation by a light pulse, so we will take:

$$T_{\mu\nu}^{\text{mat}} = 0 \text{ et } T_{\mu\nu}^{\text{em}} = -\sigma_{\mu\nu} \quad (6)$$

Where $\sigma_{\mu\nu}$ is the Maxwell stress-energy tensor in 4×4

dimension, symmetrical such that in SI notation [15]:

$$-\sigma_{00} = \epsilon_0 \frac{E^2 + c^2 B^2}{2} \quad (7)$$

the energy density.

$$-\sigma_{0k} = -\sigma_{k0} = \frac{\epsilon_{ijk} E_i B_j}{c \mu_0} \quad (8)$$

the energy flux in the direction x^k ($k = 1, 2, 3$).

$$\sigma_{ij} = \epsilon_0 E_i E_j + \frac{B_i B_j}{\mu_0} - \delta_{ij} \epsilon_0 \frac{E^2 + c^2 B^2}{2} \quad (9)$$

the 3D Maxwell constrain tensor.

With $i, j, k = 1, 2, 3$ the spatial components' indices and δ_{ij} the Kronecker symbol.

Armed with equations (5) and (6) which predict a deformation of the space-time in the presence of an electromagnetic field, we can study the gravitational perturbation generated by a light pulse propagating in an initially flat space-time.

Let us take the example of a plane progressive wave of linear polarisation traveling towards positive z axis:

$$\begin{aligned} \mathbf{E} &= E \mathbf{e}_x \text{ and } \mathbf{B} = B \mathbf{e}_y \\ E &= cB \end{aligned} \quad (10)$$

The tensor $\sigma_{\mu\nu}$ can then be written as:

$$\sigma_{\mu\nu} = -\epsilon_0 \begin{pmatrix} E^2 & 0 & 0 & E^2 \\ 0 & 0 & 0 & 0 \\ 0 & 0 & 0 & 0 \\ E^2 & 0 & 0 & E^2 \end{pmatrix} \quad (11)$$

We are thus expecting a longitudinal deformation of spacetime $h_{\mu\nu}$ by a progressive electromagnetic wave:

$$h_{00} = h_{03} = h_{30} = h_{33} = h \quad (12)$$

$$h_{\mu\nu} = 0 \text{ for } \mu \neq 0, 3 \text{ or } \nu \neq 0, 3 \quad (13)$$

This deformation profile is to be contrasted with that of the commonly studied gravitational waves, which propagate at long distances only in deformations transverse to their propagation [16].

Let us clarify the source E^2 present in the d'Alembert equation (5):

$$E = E_0 \cos(k(z - ct)) \quad (14)$$

Where E_0 is the amplitude of the wave's electric field, and $k = 2\pi/\lambda$ the wave vector of the electromagnetic wave propagating towards positive z .

Hence with equation (11):

$$\square h = -2\chi \epsilon_0 E_0^2 \cos^2(k(z - ct)) \quad (15)$$

$$\square h = -\chi \epsilon_0 E_0^2 (1 + \cos(2k(z - ct))) \quad (16)$$

We can then decompose the source term into its con-

stant part and its oscillating part, and solve these two parts separately since the d'Alembertian is a linear operator. We are only interested here in solving the linearized Einstein equation (16) for the constant part of the source term. This equation can be rewritten as:

$$-\square h = 2\chi Source \quad (17)$$

where $Source = \epsilon_0 E_0^2/2$ is the mean energy density of the light pulse. We investigate the solution of Equation (17) for a light pulse of finite spatial and temporal extension, such as it could be emitted by a laser system. This light pulse will be modeled by a cylinder of constant energy density of length L and radius R moving at the speed of light c in the direction of positive z . We propose to study an intermediate case, that of the static cylinder, in order to illustrate in a simpler case the methods used and to verify the compatibility of our method of resolution with the well known solution of the metric of Schwarzschild [13] for a stationary isolated mass.

III. RESOLUTION IN THE SIMPLE CASE OF A STATIC CYLINDER

Equation (17) is a partial differential equation on 4 dimensions. The solution of the homogeneous equation is the set of functions of $\rho - ct$ or $\rho + ct$, where ρ is the position vector of a point in space only. Since the particular solution of this equation is not apparent, we have to use Green's function G_{\square} of the d'Alembertian operator to determine a solution.

$$\square G_{\square}(\mathbf{x} - \mathbf{x}') = \delta(\mathbf{x} - \mathbf{x}') \quad (18)$$

and

$$h(\mathbf{x}) = \int_{\mathbb{R}^4} d\mathbf{x}' G_{\square}(\mathbf{x} - \mathbf{x}') Source(\mathbf{x}') \quad (19)$$

Where \mathbf{x} is the observer's time space position vector and \mathbf{x}' another vector describing a position in spacetime. Thankfully, the d'Alembertian's Green function is well-known [17] and can be written in spherical coordinates

for a retarded potential as:

$$G_{\square}(c(t - t'), |\rho - \rho'|) = -\frac{\delta(c(t - t') - |\rho - \rho'|)}{4\pi|\rho - \rho'|} \quad (20)$$

We can then focus on solving the successive integrals of Equation (19). As the following calculation highlights some techniques, we will pass by the example of a cylinder of constant energy density to illustrate them.

We represent the theoretical physical situation in Figure 1. We will here take a cylinder of radius R and length L so that the axis Oz is the axis of symmetry of the cylinder. The cylinder starts on this axis at $z = 0$ and ends at $z = L$. This cylinder appears at time $t = 0$ in a previously planar space-time. It generates a deformation which must be, at long time and far from the source, the one described by Newtonian physics for an object of equivalent mass density $\rho = \mathcal{A}/c^2$. For this cylinder of homogeneous energy density, we have the following:

$$Source(ct, z, r) = \mathcal{A}H(ct)H(z)H(L - z)H(R - r). \quad (21)$$

Where \mathcal{A} is the constant energy density inside the cylinder, and $H(z)$ is the Heaviside function. We can then

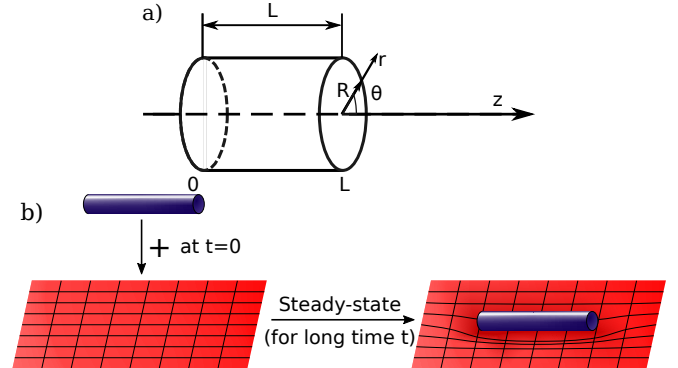


FIG. 1. a) Schematic representation of the studied static cylinder of energy density and b) Presentation of the thought experiment modeling the establishment of the gravitational potential of said cylinder at $t = 0$ and $t \gg 0$.

rewrite Equation (19) in cylindrical coordinates. Taking into account that, in Equation (20) we have $|\rho - \rho'| = \sqrt{(z - z')^2 + (r^2 + r'^2 - 2rr' \cos\theta')}$, we get:

$$h(ct, z, r, \theta) = \frac{2\chi}{4\pi} \int_{-\infty}^{\infty} c dt' \int_{-\infty}^{\infty} dz' \int_0^{\infty} r' dr' \int_0^{2\pi} d\theta' Source(ct', z', r', \theta') \frac{\delta(c(t - t') - |\rho - \rho'|)}{|\rho - \rho'|} \quad (22)$$

$$h(ct, z, r, \theta) = \frac{\chi}{2\pi} \int_{-\infty}^{\infty} dz' \int_0^{\infty} dr' \int_0^{2\pi} d\theta' Source\left(ct - \sqrt{(z - z')^2 + (r - r')^2}, z', r', \theta'\right) \quad (23)$$

$$\times \frac{r'}{\sqrt{(z - z')^2 + (r^2 + r'^2 - 2rr' \cos\theta')}}$$

For the sake of simplicity, we only calculate the gravitational influence of the cylinder on the Oz axis, the axis of symmetry of the cylinder. We thus have $r = 0$, which leads us to note $h(ct, z, r, \theta) = h(ct, z)$. By introducing Equation (21), we then obtain:

$$h(ct, z) = \frac{\chi\mathcal{A}}{2\pi} \int_{-\infty}^{\infty} dz' H(z') H(L - z') \times \quad (24)$$

$$\int_0^{\infty} H(ct - \sqrt{r'^2 + (z' - z)^2}) H(R - r') \frac{r' dr'}{\sqrt{(z - z')^2 + r'^2}}$$

]

$$h(ct, z, 0) = \mathcal{A}\chi \int_{-\infty}^{\infty} dz' H(z') H(L - z') H(z' - (z - ct)) H((z + ct) - z') \underbrace{\left[-\sqrt{(z - z')^2} \right]}_{\text{lower integration bound}} + H\left(\sqrt{c^2 t^2 - (z - z')^2} - R\right) \underbrace{\left[\sqrt{(z - z')^2 + R^2} + H\left(R - \sqrt{c^2 t^2 - (z - z')^2}\right) ct \right]}_{\text{upper integration bound}} \quad (26)$$

The integration can be carried out "by hand", but the analytical solution is difficult to interpret. It is therefore preferable to linearize the conditions on z' , find the functions' primitives, and provide them to a Python program [18] that will compare the different terms and conditions to plot the solution of Equation (26).

IV. VISUALISATION AND STUDY OF THE ANALYTICAL SOLUTION

In order to model what a current petawatt-class power laser could produce [19], we take the following values: $\mathcal{A} \times c = I = 10^{22} \text{ W/cm}^2$, $E = 525 \text{ J}$ which correspond to the following dimensions of the static cylinder: $L = 20 \mu\text{m}$, $R = 5 \mu\text{m}$. The solution is shown in Figure 2. This visualization highlights the establishment (zone I and II) of the stationary solution (zone III) for the gravitational deformation of a static cylinder of constant energy density. We thus have the exact solution for an out of equilibrium space-time, a point which will be very useful for the study of the cylinder moving at the speed of light.

This transient regime leads to a stationary deformation in time which corresponds to a gravitational potential. The stationary potential thus established in zone III is the gravitational potential of the cylinder of stationary energy density. This potential is the strict analogue of the potential which would be generated by a massive object of cylindrical shape along its axis. This potential behaves at long distance as $1/z$, i.e. like the gravitational potential of a massive object at long distance. Indeed let us take for example z large and negative, in order to

Heaviside functions exhibit conditions for integration. Among these conditions, the condition to linearize with respect to r' to perform the integration is:

$$ct - \sqrt{r'^2 + (z' - z)^2} \geq 0 \Rightarrow \begin{cases} r'^2 \leq c^2 t^2 - (z' - z)^2 \\ c^2 t^2 - (z' - z)^2 \geq 0 \end{cases} \quad (25)$$

By studying the different conditions, we reach the expression:

$$\begin{aligned} h(z, L, R) / \chi\mathcal{A} &= \\ &= -L(L - 2z) + (L - z)\sqrt{R^2 + (z - L)^2} + \\ &+ R^2 \text{arcsh} \left(\frac{L - z}{R} \right) + z\sqrt{R^2 + z^2} - R^2 \text{arcsh} \left(\frac{-z}{R} \right) \\ &\approx \frac{LR^2}{-z} \end{aligned} \quad (27)$$

Be careful, here the potential thus generated is positive, for $-z$ is positive. We therefore find a potential similar to the $1/r$ gravitational potential found in Schwarzschild [13]'s metric model.

If we study cylinders of different aspect ratios L/R at constant I and E , it appears that the maximum gravitational deformation on the Oz axis varies. This maximum is plotted as a function of the aspect ratio Figure 3. The abscissa of the maximum of gravitational deformation as a function of the aspect ratio Figure 3 cannot be explained only by a geometrical argument, we will stop there in the study of the case of a static cylinder, which already gives us a reliable result. In our example the maximum of the perturbation h is 8×10^{-37} for $L/R \sim 1.77$ with $I = 10^{22} \text{ W/cm}^2$ and $E = 525 \text{ J}$. Armed with the observations made and the tools developed in this section, we will extend this study to the more realistic case of a cylinder of light moving at the speed of light c .

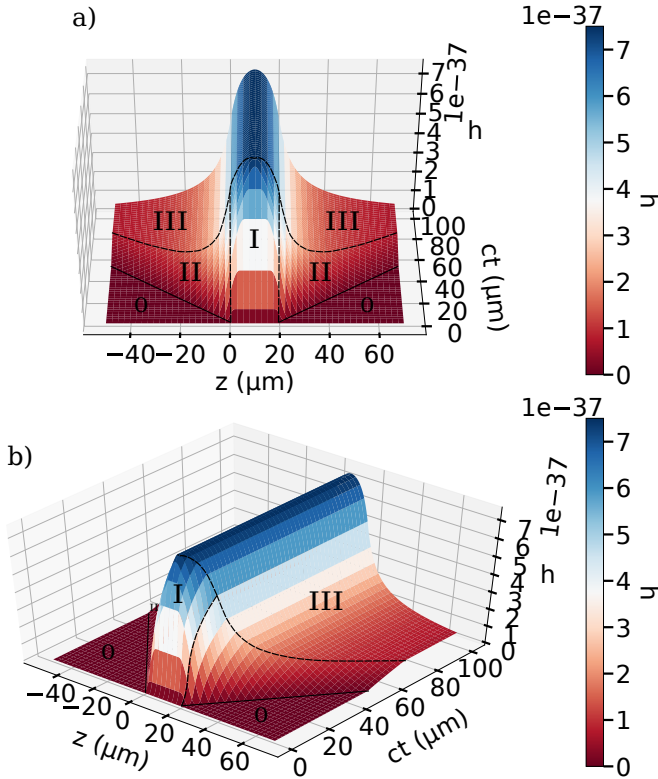


FIG. 2. 3D representation according to two angles (a) "head-on" and b) "front-on") of the solution on the plane (O, z, ct) for a laser intensity $I = 10^{22} \text{ W/cm}^2$ and dimensions of the light cylinder $L = 20 \mu\text{m}$, $R = 5 \mu\text{m}$. The numbers indicate the solution's regimes. Zone I: the transient regime inside the source, zone II: the transient regime outside the source, zone III: the permanent regime, zone 0: unperturbed spacetime.

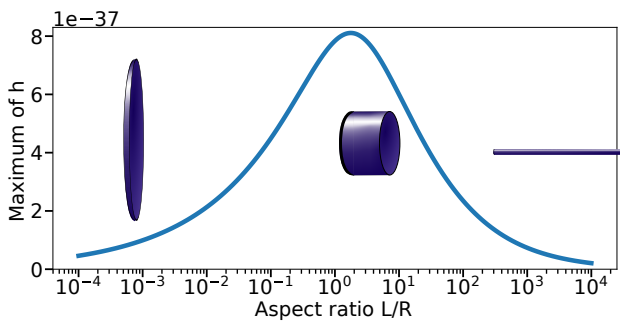


FIG. 3. Maximum amplitude of the gravitational deformation h generated by a cylinder of constant energy density $\mathcal{A} = 3.3 \times 10^{11} \text{ W/cm}^3$ and constant energy $E = 525 \text{ J}$ as a function of the aspect ratio L/R of the cylinder. The 3 cylinders represent the general shape of the cylinder for the different aspect ratio domains in the figure.

V. LIGHT PULSE MODEL: CYLINDER MOVING AT SPEED C

We repeat here the method presented previously for a static cylinder. We now consider the cylinder of light moving at the speed of light c . This problem is illustrated in Figure 4. This cylinder moves in the direction of positive z in such a way that the cylinder of light is located at time t between $z = ct$ and $z = ct + L$. It appears at $t = 0$ in a planar space-time. The energy density in spacetime can therefore be written as:

$$\text{Source}(ct, z, r, \theta) = \mathcal{A}H(ct)H(R - r)H(r)H(z - ct)H(L - (z - ct)) \quad (28)$$

A first rough analogy would be to compare this case of a longitudinal deformation propagating at the same speed as the object that generates it with the already known case of an object moving at the speed of sound in a medium. This analogy highlights the particularity of a case where the source and the perturbation propagate at exactly the same speed as compared to another case simply moving at any speed, as well as the interest that such a phenomenon would have in obtaining an important gravitational deformation. An illustration of the difference between these two cases is proposed in Figure 4b.

Note: In any other case where the cylinder moves at

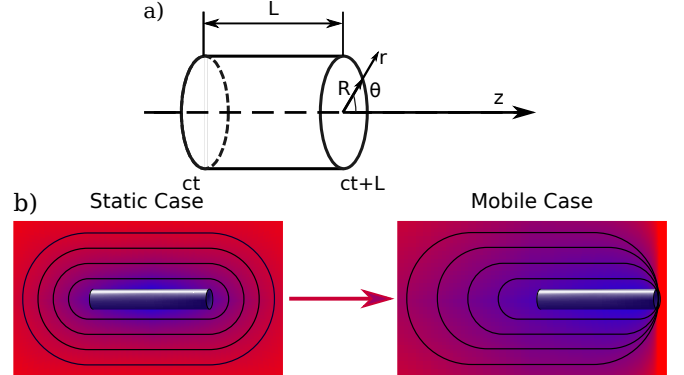


FIG. 4. a) Schematic representation of the cylinder of uniform energy density moving at the speed of light and b) Illustration of the expected differences between the gravitational deformation generated by the static cylinder previously studied and that generated by a light pulse of the same cylindrical shape.

speed $v < c$, one could have applied a Lorentz transform to the static case in order to take into account the new relative speed of the cylinder. However, this transform produces divergent values for $v = c$. We cannot use the Lorentz transform, so it is imperative to solve the problem by convolution product of the $\text{Source}(ct, z, r)$ term with the D'Alembertian Green function.

In order to simplify the calculations, we will place our-

selves in the comoving frame of reference in respect to the cylinder of light, that is to say:

$$(O, ct, z, z') \mapsto (O, ct, Z, \tilde{z}) \text{ such as: } \begin{cases} Z = z - ct \\ \tilde{z} = z' - z \end{cases} \quad (29)$$

We take the expression of the solution given by the expression (23), and we now introduce the source term corresponding to a cylinder of light moving at c :

$$h(ct, z) = \mathcal{A}\chi \int_{-\infty}^{\infty} d\tilde{z} \int_0^{\infty} H(ct - \rho_0) H(\tilde{z} + Z + \rho_0) H(L - Z - \tilde{z} - \rho_0) H(R - r') \frac{r' dr'}{\rho_0} \quad (30)$$

Where $\rho_0(r', \tilde{z}) = \sqrt{\tilde{z}^2 + r'^2}$. Which leads us, by the same reasoning as the one presented in part III, to:

$$h(t, z, 0) = \mathcal{A}\chi \int_{-\infty}^{\infty} d\tilde{z} H(\tilde{z} + ct) H(ct - \tilde{z}) H(L - Z) H(L - Z - \tilde{z}) \times \\ \times \left[\begin{array}{l} \text{upper} \quad \left\{ \begin{array}{l} H(c^2 t^2 - (L - Z - \tilde{z})^2) H(c^2 t^2 - \tilde{z}^2 - R^2) \frac{ct}{(L - Z - \tilde{z})} \\ + H((L - Z - \tilde{z})^2 - c^2 t^2) H((L - Z - \tilde{z})^2 - \tilde{z}^2 - R^2) (L - Z - \tilde{z}) \\ + H(c^2 t^2 - R^2) H((L - Z - \tilde{z})^2 - R^2) \sqrt{R^2 + \tilde{z}^2} \end{array} \right. \\ \text{integration} \quad \left. \right. \\ \text{bound} \quad \left. \right. \end{array} \right. \\ \left. - \underbrace{H(-Z) H(-Z - 2\tilde{z}) (-Z - \tilde{z}) - (H(Z) + H(-Z) H(Z + 2\tilde{z})) |\tilde{z}|}_{\text{lower integration bound}} \right] \quad (31)$$

To which equation follows a calculation step applied to a Python program having the same function of solution representation as the one presented part III.

VI. RESULTS AND ANALYSIS

A. Study at constant intensity and energy

In order to model again what could be obtained with a current ultra high power laser [19], we take again as characteristics $I = \mathcal{A} \times c = 10^{22} \text{ W/cm}^2$, $E = 525 \text{ J}$, which still correspond to the dimensions $R = 5 \mu\text{m}$ and $L = 20 \mu\text{m}$. The Python program then gives us the visualization shown in Figure 5. The gravitational perturbation generated by a cylinder of light moving at speed c has a characteristic "wave" profile, instead of the symmetrical profile we had in the static case. Indeed, the fact that we place ourselves in the comoving frame implies that, by causality, no perturbation can be present "in front of" the source, i.e. for $Z > L$. The maximum is located at the comoving coordinate $Z = 0$ in a rather logical way. Indeed, any perturbation generated in the source at a comoving coordinate Z_1 cannot be observed at a later time at a point of comoving coordinate $Z_2 > Z_1$, because the opposite would imply that a perturbation has moved faster than the speed of light. Still, we keep a $1/Z$ shaped potential in the "trail" of this wave (zone III). Among the differences that can be observed between the static case and this new mobile case, is the growth

of the disturbance in the source, which instead of reaching a stationary regime after a certain time, seems to continue to grow in zone I. Indeed, a logarithmic growth now seems to appear after the first growth phase that we could already observe in the static case. This growth can be easily isolated in the different terms of contribution to the perturbation. Thus for $Z = 0$, at long times such that $ct \gg R$ and $R \gg L$, one can isolate as the only contribution to the perturbation the following terms:

$$h = \frac{\chi\mathcal{A}}{2} \left(\frac{R^2}{2} + R^2 \left[\operatorname{arcsh} \left(\frac{L}{2R} - \frac{R}{2L} \right) + \operatorname{arcsh} \left(\sqrt{\frac{c^2 t^2}{R^2} - 1} \right) \right] + ct \left(ct - \sqrt{c^2 t^2 - R^2} \right) \right) \quad (32)$$

Which nets us through a Taylor expansion:

$$h \approx \frac{\chi\mathcal{A}R^2}{2} \left[1 + \ln \left(\frac{4Lct}{R^2} \right) \right] \quad (33)$$

In order to supplement this expansion carried out for a limited domain of space-time, we will again be interested in the impact of the shape of the cylinder on the amplitude at a given time of this deformation. The goal is finally to find the optimal configuration to generate the largest possible deformation. For this, we will study the profile of the maximum of this deformation, located at $Z = 0$ for several aspect ratios, as shown in Figure 6. We observe that each maximum of gravitational deformation seems to evolve in time according to two modes of growth: in a first period of time, the perturbation sees an accel-

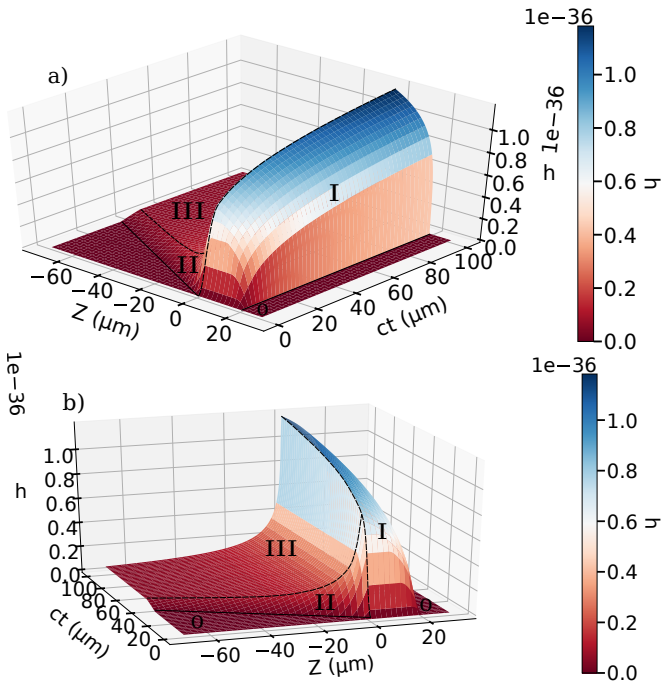


FIG. 5. 3D representation according to two angles (a) "from the front" and b) "from the back") of the solution on the comoving plane (O, Z, ct) for a laser intensity $I = 10^{22} \text{ W/cm}^2$ and dimensions of the light cylinder $L = 20 \mu\text{m}$, $R = 5 \mu\text{m}$. Zone I/ the growth regime inside the source, zone II/ the transient regime outside the source, zone III/ the quasi-static regime outside the source and zone 0/ unperturbed spacetime.

eration of its growth (in the broad sense, this growth is at least linear), followed by a second period, with longer times, where the growth becomes logarithmic. The duration of this first period of time is different for each aspect ratio, and appears to occur later and later as the aspect ratio decreases. Thus, the cylinder of light with the second largest aspect ratio ($L = 18 \mu\text{m}$, $R = 5.3 \mu\text{m}$), initially generates the highest maximum. But the slowing of its growth at longer times means that at $ct = 50 \mu\text{m}$ the largest deformation maximum is possessed by another cylinder of light ($L = 1.9 \mu\text{m}$, $R = 16.2 \mu\text{m}$). By the same logic, the cylinder of light with the smallest aspect ratio ends up catching up with the previous cylinder in terms of maximum generated perturbation. We must therefore expect to see the optimal aspect ratio of the cylinder of light, i.e. the one which gives the greatest gravitational perturbation on the axis, move towards the small aspect ratios as time increases. This hypothesis is confirmed by plotting the maximum perturbation at a given time as a function of the aspect ratio in Figure 7. We can observe on this occasion that the maximum of deformation increases with time in a way that cannot only be explained by the logarithmic growth highlighted earlier. It seems that taking a cylinder of light of larger radius, and therefore of smaller length at constant intensity and energy, favors the generation of a larger gravi-

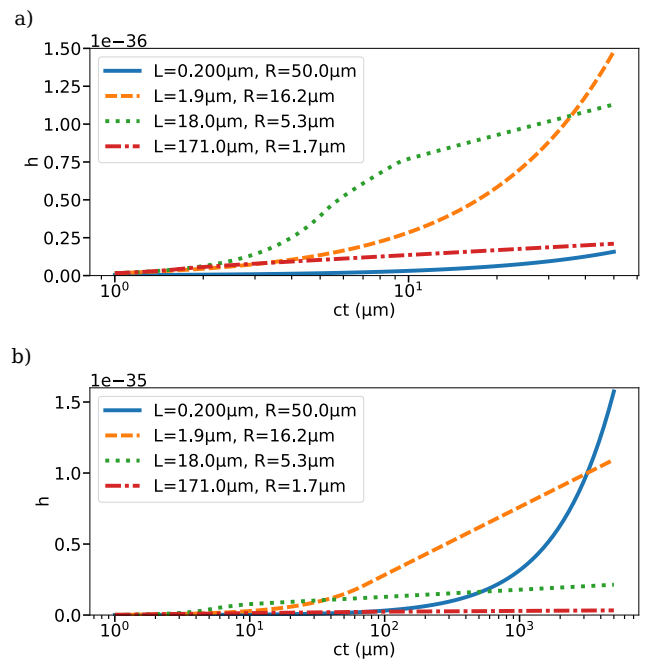


FIG. 6. Detail of the growth of the maximum of gravitational perturbation until the time such as a) $ct = 50 \mu\text{m}$ b) $ct = 5 \text{ mm}$. This perturbation is generated by a cylinder of intensity $I = 2 \times 10^{22} \text{ W/cm}^2$ and energy $E = 525 \text{ J}$ as a function of time for cylinders with various aspect ratios.

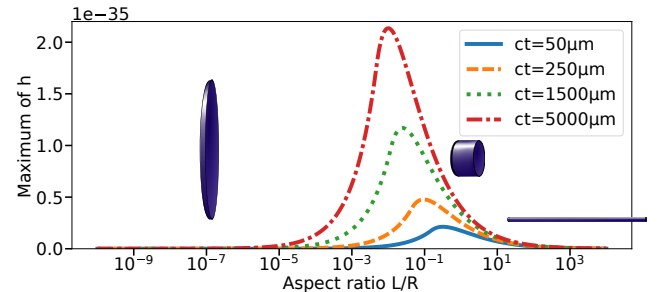


FIG. 7. Maximum amplitude at fixed time of the gravitational perturbation generated by a cylindrical light pulse of intensity $I = 2 \times 10^{22} \text{ W/cm}^2$ and energy $E = 525 \text{ J}$ according to the aspect ratio L/R of said cylinder.

tational perturbation. This can be explained by the fact that such a "light disk" has at long times more source points, and thus emitting points, close to the observation point in $Z = 0$ at the time of the observation.

Thus, in an ideal setting where one could make a light pulse propagate as a cylinder of energy density over an indefinite time, the intensity plays an important role since the amplitude grows linearly with it. Nevertheless, another way to maximize the gravitational deformation at constant intensity could also be to let the perturbation

grow by letting the light propagate as long as possible, under the explicit condition of adjusting the aspect ratio of the cylinder to the distance traveled to have the best efficiency. The amplitude of this deformation will be limited by the length on which we can experimentally focus the beam.

This deformation's front has a peculiar wave shape, which ensures a strong instantaneous variation of the metric when the gravitational deformation would reach the observer. Now the variations of the metric are responsible for some of the effects observable in gravity potentials, as the deflection of light. The deformation's profile has therefore interesting properties for the measurement of a gravitational perturbation generated in the laboratory.

B. Study at constant power

Most laser facilities propose lasers with a fixed maximum power. We must therefore observe the dependence of the gravitational deformation on power. In this case, at constant power, L does not change the intensity of the beam, since $P = \pi R^2 I$. We will however represent the deformation at different L , to check if the change of aspect ratio has an influence on the observed deformation. Equation (33) seems to show that at long time for $R \gg L$ the solution could be proportional to IR^2 and thus to the power P .

If this proportionality is proven in a more global framework, we would end up with a parameter to be adjusted, the power, not requiring the extreme focusing of the laser beam and thus avoiding the complications arising with very high intensity light beams.

At fixed time the maximum of gravitational perturbation seems to decrease when the radius increases, as presented in Figure 8. This result may seem at first sight contradictory to the result of Equation (33), but two differences must be taken into account here. The plots are done at constant time, as the radius R of the cylinder is what varies. Now, the equation includes a term $\ln(4L/R^2)$ which decreases as R increases. But there is also a radius R from which we no longer have $ct \gg R$ and where the Taylor expansion is no longer valid. At large R 's, we can relate this decrease to the relation $I = P/(\pi R^2)$. Indeed, R being larger than ct , the deformation generated by the edges of the cylinder could not yet reach the center of the cylinder. So we only decrease the intensity of the beam without really increasing the volume of contributions. However, in a situation closer to physical reality, a light beam does not remain cylindrical *ad eternam*. It can only be considered cylindrical over twice its Rayleigh length, that is, twice the distance it takes for a focused beam to diffract and see its radius multiplied by $\sqrt{2}$. This distance depends of course on how focused the beam is, as well as its wave-

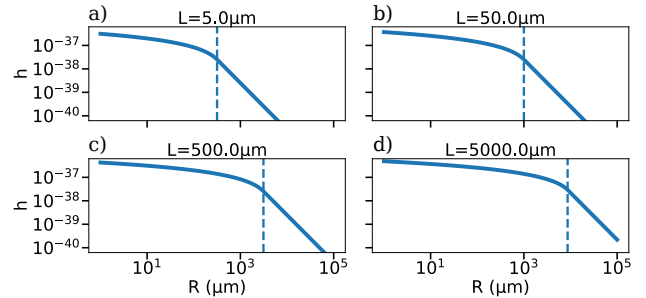


FIG. 8. Maximum of amplitude at time such that $ct = 1$ cm of the gravitational perturbation of a cylindrical light pulse of fixed length L (i.e. at fixed time) (a) $L = 5 \mu\text{m}$, b) $L = 50 \mu\text{m}$, c) $L = 500 \mu\text{m}$, d) $L = 5000 \mu\text{m}$) and of constant power $P = 1 \text{ PW}$ as a function of the radius R of the cylinder.

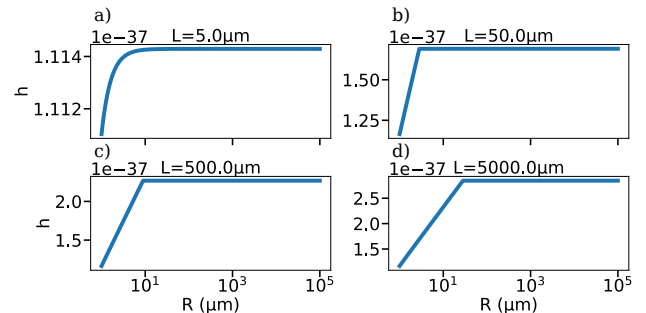


FIG. 9. Maximum of amplitude at set L (a) $L = 5 \mu\text{m}$, b) $L = 50 \mu\text{m}$, c) $L = 500 \mu\text{m}$, d) $L = 5000 \mu\text{m}$) of the gravitational deformation at constant power $P = 1 \text{ PW}$ as a function of the cylinder radius R and at time such that $ct = 2 z_r$

length, according to the designated formula:

$$z_r = \frac{\pi R^2}{\lambda} \quad (34)$$

Where z_r is the Rayleigh length, R the minimum radius of the beam, and λ the focused light's wavelength. This quantity thus introduces an upper limit on the propagation time of the cylinder of light, which is $t_r = 2z_r/c$. There is therefore a direct link between the maximum propagation time and the radius R of the cylinder. If we consider that we want the largest possible perturbation of the gravitational field, we can then consider that any cylinder of light that we study generates a gravitational perturbation over the longest possible time, that is t_r . We can then re-study the results at constant power, as a function of R , such that the cylinder of light has generated a gravitational deformation over $2z_r$. This new calculation which takes more into account the experimental situation, and presented in Figure 9, shows that the in-

crease of the cylinder radius is far from being detrimental, contrary to what was previously thought. As long as the radius R is sufficiently large compared to the length L of the cylinder, the gravitational deformation generated by a cylinder of light is indeed constant at constant power.

Taking Equation (33) and introducing t_r , we then obtain:

$$h \approx \frac{\chi P}{2c} \left[1 + \ln \left(\frac{8\pi L}{\lambda} \right) \right] \quad (35)$$

This last expression is, at constant power P , independent of R and logarithmically dependent on the ratio L/λ . These results confirm, in particular, that the determining physical quantity for the gravitational deformation is the power P of our light beam. In practice, this very important result allows us to get rid of the need for a very focused light beam, and thus of the quantum electrodynamics effects appearing at ultra high intensities. It also allows us to have experiment sizes that can be calibrated to the detection method used.

VII. CONCLUSION

The study of the gravitational deformation generated by the constant part of the electromagnetic stress-energy tensor $T_{\mu,\nu}^{em}$ of a light pulse gives us several important results. First we have put into action a case exhaustion method in order to obtain an analytical solution for the Einstein equations with a source delimited in space. It has been proved to give at long distances the result expected from the Schwarzschild [13] model for a static cylinder of constant energy density, and gave us more insight on the establishment of such a gravitational deformation in the frame of the thought experiment of a suddenly appearing amount of energy. This method will prove useful in the calculation of further physical cases, including the study of the oscillatory term in Equation (16).

The gravitational perturbation generated by a cylinder of constant energy density moving at the speed of light c presents a singular profile. This wave-like profile along z gives us good hopes for the study of the detection of the deformation by a probe beam, since the light deflection depends on the variation of the metric.

Finally, the value of gravitational deformation h found for a beam of power $P = 1$ PW is of the order of 10^{-37} , which is still small but shows an improvement compared to the generation of a gravitational perturbation by matter acceleration. To recall the results of theorized experiments for generation by mass acceleration, the paper by Ribeyre and Tikhonchuk [5] presents the different possible methods of generating gravitational deformation by mass ablation by high power laser. They give an evaluation of the value of such a deformation for each of the different experiments performed for powers of the order

of a PW or energies of the order of a MJ. For these values, they find a deformation of the order of:

$$h_m \approx 10^{-40} \sim 10^{-39} \quad (36)$$

The main limiting factor to these results is the distance at which the observing device must stand due to the explosive nature of the mass acceleration. Ribeyre and Tikhonchuk [5] position in this paper such a detection device at 10 m from the source, a huge distance compared to those considered for the study of the direct generation of a gravitational deformation by intense light.

The results of Kadlecová *et al.* [7] confirm this evaluation by finding for the studied experiment:

$$h_m \approx 5 \times 10^{-40} \quad (37)$$

These results shall be put in perspective with the result of this study, which gives us a ratio of at least two orders of magnitude between the deformation generated by mass acceleration and that generated by intense light of:

$$\frac{h}{h_m} \approx 200 \quad (38)$$

Note the qualitative difference between the nature of the gravitational deformation created by mass acceleration compared to that created by a beam of light that we have studied here.

While the first one is of chaotic nature because of the intense and arbitrary nature of the process of ejection and propulsion of mass by the creation of a plasma, the second one is directly generated by a laser, that is to say an object with well determined geometrical properties. Grishchuk [9] puts forward in his paper this case of establishment of a coherent gravitational source, compared to a generation by mass acceleration, whose coherence would be difficult to establish and maintain.

Furthermore, gravitational waves are, on one hand, induced by the quadrupolar moment of acceleration for the massive case, which greatly reduce the efficiency of this method, and generates a deformation that is transversal to its propagation, whereas on the other hand the generation by light fully uses the displaced energy and nets us a longitudinal deformation, which constitutes another subtlety that will have to be taken into account in further experiments.

Obtaining a gravitational deformation of the order of $h = 10^{-37}$ for a laser of power $P = 1$ PW allows us to consider a source of gravitational deformation which, although still of weak effect, appears to be coherent, easier to observe and especially more adaptable to the frequency range of detection than the generation by matter acceleration. The perspectives of detection of such a gravitational wave remain to be studied. But we can already lift the veil on two interesting detection setup. One of them is the Li-Baker interferometer [20] which according to its developers could reach a minimum of detection at 10^{-37}

for gravitational deformation of frequency of the order of 10 GHz. The other would be the measure of the delay induced on an atomic clock by the repeated exposition to the gravitational deformation generated by a beam of light. The related experiment would rely on the capacity of some laser facilities to deliver high power laser pulse at relatively high frequencies, thus allowing to measure the deformation created repeatedly by the accumulation of the induced delay on an atomic clock.

Room for improvement can also be made in the laser power, as one could envision lasers who would soon reach a power in the exawatts. Due to the linear dependence of the gravitational deformation on laser power, this would lead to $h \approx 10^{-34}$. This progress could lead to one of the end goal of the generation of gravitational wave in the laboratory, which would be the establishment of the gravitational equivalent to a Hertz experiment, where we would generate and detect a gravitational perturbation.

Another physical phenomenon that could be of use in proving the validity of such a gravitational deformation generation would be the Gamma Ray Bursts (GRB). These astronomical phenomena indeed generate extremely powerful light beams $10^{44} - 10^{45}$ W for a duration up to a whole second, i.e $L = 3.0 \times 10^8$ m [21]. Considering the GRB photons have a relatively uniform en-

ergy around 250 keV, i.e $\lambda = 50$ nm, Equation (35) gives us $h \approx 10^{-6}$ as an approximate of the amplitude of the gravitational deformation inside a cylindric enough GRB. This is an impressive result which will probably need its own accurate calculation since, far from its source, a GRB's shape tends to be more conic. This result still gives great hope for the detection of gravitational deformations induced by light.

Before approaching the detection of such a wave, however, we will have to study the role, without doubt of physical significance, of the oscillating character of the light pulse that we have put aside in this article.

ACKNOWLEDGEMENTS

This research was supported by the French National Research Agency (Grant No. ANR-17-CE30-0033-01) TULIMA Project and by the NSF (Grants No. 1632777 and No. 1821944) and AFOSR(Grant No. FA9550-17-1-0382). We thank J.L. Dubois, F. Catoire and P. Gonzalez de Alaiza Martinez for the interest they've shown in this study and their advice.

[1] A. Einstein, Näherungsweise Integration der Feldgleichungen der Gravitation, *Sitzungsberichte der Königlich Preussischen Akademie der Wissenschaften zu Berlin Jan-Juni* **1916** (1916).

[2] R. A. Hulse and J. H. Taylor, Discovery of a Pulsar in a Binary System, *The Astrophysical Journal* **195**, L51 (1975).

[3] B. P. Abbott and LIGO Scientific Collaboration and Virgo Collaboration, Observation of Gravitational Waves from a Binary Black Hole Merger, *Phys. Rev. Lett.* **116**, 061102 (2016).

[4] B. P. Abbott and LIGO Scientific Collaboration and Virgo Collaboration, GW170817: Observation of Gravitational Waves from a Binary Neutron Star Inspiral, *Phys. Rev. Lett.* **119**, 161101 (2017).

[5] X. Ribeyre and V. Tikhonchuk, High Frequency Gravitational Waves Generation in Laser Plasma Interaction, in *The Twelfth Marcel Grossmann Meeting* (WORLD SCIENTIFIC, UNESCO Headquarters, Paris, France, 2012) pp. 1640–1642.

[6] E. G. Gelfer, H. Kadlecová, O. Klímo, S. Weber, and G. Korn, Gravitational waves generated by laser accelerated relativistic ions, *Physics of Plasmas* **23**, 093107 (2016).

[7] H. Kadlecová, O. Klímo, S. Weber, and G. Korn, Gravitational wave generation by interaction of high power lasers with matter using shock waves, *Eur. Phys. J. D* **71**, 89 (2017).

[8] G. F. Chapline, J. Nuckolls, and L. L. Wood, Gravitational-radiation production using nuclear explosions, *Phys. Rev. D* **10**, 1064 (1974).

[9] L. P. Grishchuk, Electromagnetic Generators and Detectors of Gravitational Waves, *arXiv:gr-qc/0306013* (2003), *arXiv:gr-qc/0306013*.

[10] F. W. Dyson, A. S. Eddington, and C. Davidson, A Determination of the Deflection of Light by the Sun's Gravitational Field, from Observations Made at the Total Eclipse of May 29, 1919, *Philosophical Transactions of the Royal Society of London* , 45 (1920).

[11] R. C. Tolman, P. Ehrenfest, and B. Podolsky, On the Gravitational Field Produced by Light, *Physical Review* **37**, 602 (1931).

[12] D. Rätzel, M. Wilkens, and R. Menzel, Gravitational properties of light—the gravitational field of a laser pulse, *New J. Phys.* **18**, 023009 (2016).

[13] K. Schwarzschild, Über das Gravitationsfeld eines Massenpunktes nach der Einsteinschen Theorie., *Sitzungsberichte der Königlich Preussischen Akademie der Wissenschaften zu Berlin* (1916).

[14] L. D. Landau and E. M. Lifshitz, *The Classical Theory of Fields*, 4th ed., Course of Theoretical Physics No. by L. D. Landau and E. M. Lifshitz ; Vol. 2 (Elsevier [u.a.], Amsterdam [u.a], 2009).

[15] J.-C. Boudénot, *Electromagnetisme et Gravitation Relativistes* (1989).

[16] M. Maggiore, *Gravitational Waves*, Vol. 1: Theory and Experiments (2008).

[17] J. D. Jackson, *Classical Electrodynamics*, 3rd ed. (Wiley, New York, 1999).

[18] The code used to visualize the solutions is accessible in Paul Lageyre's github repository: https://github.com/Paul-Lageyre/2021_plotting_code.

- [19] C. N. Danson et al., Petawatt and exawatt class lasers worldwide, *High Pow Laser Sci Eng* **7**, 10.1017/hpl.2019.36 (2019).
- [20] R. M. L. Baker, The Li-Baker High-Frequency Relic Gravitational Wave Detector (2010).
- [21] T. Piran, The physics of gamma-ray bursts, *Rev. Mod. Phys.* **76**, 68 (2004).